ARCHIVES OF ACOUSTICS
**33**, 3, 351–362 (2008)

# DYNAMIC MEASUREMENT OF PARTICLE DIAMETER AND DRAG COEFFICIENT USING THE ULTRASONIC METHOD

Hans-Dieter SOMMERLATT[(1)], Artur ANDRUSZKIEWICZ[(2)]

[(1)] TU Dresden, Institute of Fluid Mechanics
Chair of Magnetofluiddynamics
01062 Dresden, Germany

[(2)] Wrocław University of Technology
Institute of Power Engineering and Fluid Mechanics I-20
Wybrzeże Wyspiańskiego 27, 50-370 Wrocław, Poland
e-mail: Artur.Andruszkiewicz@pwr.wroc.pl

(*received November 05, 2007; accepted May 20, 2008*)

The possibility of ultrasonic impulse echo method utilization for diameter determination in liquids and for frontal drag coefficient calculation has been presented in this paper. The investigations were carried out in uniform and accelerated motion area for steel and glass balls freely falling in a water-filled tank. The accuracy of this method as a function of flight time readout resolution and ultrasonic wave velocity equation, assumed for calculations has been analyzed as well. Its further utilization in two-phase liquid metal/gas flow investigations has been proposed in this paper.

**Keywords:** ultrasonic impulse echo method, spherical particles diameter, frontal drag coefficient, measurement error, uncertainty.

## 1. Introduction

Proper determination of the bubbles dimension and their frontal drag coefficient is one of the necessary tasks required for liquid/gas or liquid metal/gas, two-phase flow identification. Proper values of these variables are indispensable for optimizing processes where these flows play an important role, and for mathematical procedures identification as well, used in theoretical research for these flows. According to ORZECHOWSKI *et al.* [1], the process of gas bubbles generation is extremely difficult to be theoretically described and approximate empirical equations are used for these bubbles diameter determination. Basic equations for bubble diameters calculation are summarized in the paper about bubble columns by KANTARCI *et al.* [2]. The Mersmann's theoretical equation, obtained from balance of the forces exerted on a single, spherical gas

bubble, is the one most often used in practical applications (e.g. KAISER [3, 4] for calculating the diameter of the argon bubbles climbing in liquid metals, Hg and GaInSn). Another way considers gas bubble equivalent diameter calculation from the bubble generation frequency [1]. For several years, the authors of this paper have been conducting the research work, within the SFB 609 Project, "Elektromagnetische Strömungsbeeinflussung in Metallurgie Kristallzüchtung und Elektrochemie (MFD- Zweiphasenströmungen)", at the TU Dresden – Institut für Strömungsmechanik, concerning the application of ultrasonic/pulse echo method for liquid/gas two-phase flows identification. The details of the method, have been described elsewhere [5, 6].

The main purpose of this paper is to investigate the potential application of this method for diameter measurement of spherical particles moving down in a liquid. The experiments were carried out for steel and glass balls of various sizes, freely falling in water-filled tank. In the process of the balls speed determination it was possible to calculate the frontal drag coefficient values as well. The method accuracy analysis would allow, in further stages of the SFB 609 Project, to use it directly for dimensions and drag coefficients determination of gas bubbles (spherical, elliptic) moving up in liquid metals.

## 2. Principle of measurement

The measurement principle is based on ultrasonic USIP 20 GP8 flaw detector. An exemplary echograph in form of a type A image is shown in Fig. 1. Short pulses transmitted from ultrasonic sensor, after they go through the tank wall, are reflected from

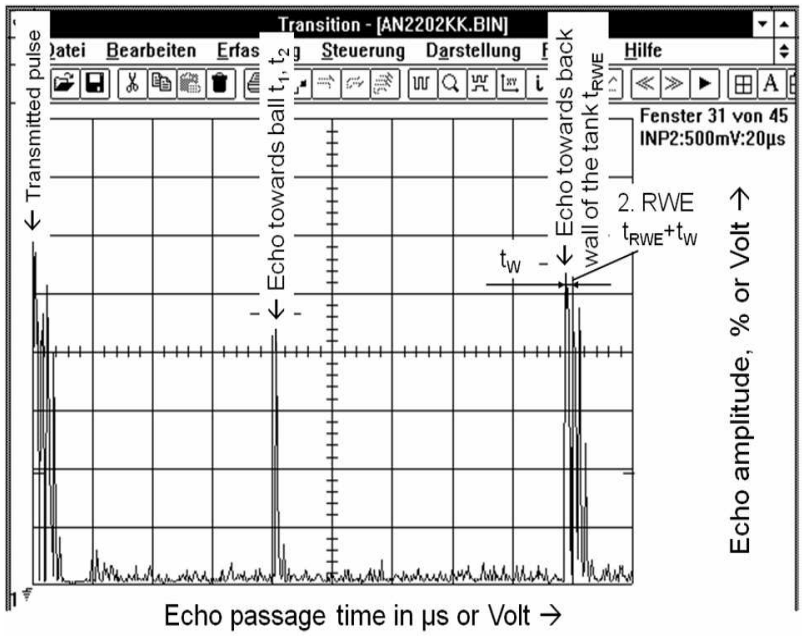


Fig. 1. Measuring principle for pulse echo method and ultrasonic flaw detector, type USIP 20 GP8: $t_W$ – time of flight through tank wall.

the falling ball ($t_1$) and back walls of the tank ($t_{\text{RWE}}$), ($t_{\text{RWE}} + t_W$), and then they are returned to the sensor. Defectoscope records signals with amplitudes higher than the preset value only, on an average, amounts to 20% of the maximum scale on the monitor screen.

Basing on the time of flight, $t_1$ and $t_2$, from the ball falling down to the ultrasonic sensors installed at the same measuring height on opposite sites of the tank, and time of flight, $t_{\text{RWE}}$, $t_{\text{RWE}} + t_W$, from rear walls of tank, and also the velocity of ultrasonic wave in water, $c_{\text{H}_2\text{O}}$, the diameter of freely falling ball, $d_K$, are calculated by means of Eqs. (1) and (2):

$$t_K = t_{\text{RWE}} + t_W - (t_1 + t_2), \tag{1}$$

$$c_{\text{H}_2\text{O}} = 2d_K/t_K. \tag{2}$$

When we then denote $t_{2.\text{RWE}} = t_{\text{RWE}} + t_W$, time $t_K$ is given by:

$$t_K = t_{2.\text{RWE}} - (t_1 + t_2). \tag{3}$$

Application of ultrasonic flaw detector enables direct determination of the passage time for the second echo ($t_{2.\text{RWE}}$), reflected from the external back wall of the tank. Such procedure causes that one variable in the measurement uncertainty analysis, i.e. ($t_W$) – the time of flight through tank wall – is thus eliminated which reduces the value of error of ball diameter calculations. The echogram from Fig. 1 illustrates also clearly the second echo (2.RWE), while Fig. 2 shows the detailed method of determining the ball diameter.

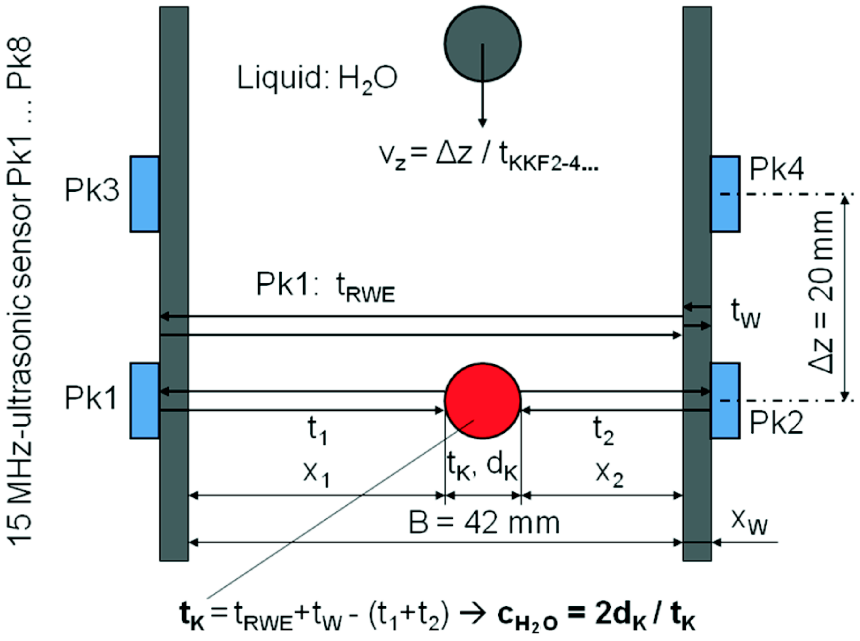


Fig. 2. Method of determining the diameter of freely falling ball.

While calculating the speed of a freely falling ball, Eq. (4) may be used at the same time to calculate the frontal drag coefficient, $c_D$:

$$c_D = \frac{4}{3} \cdot \frac{(\rho_K - \rho_{\mathrm{H_2O}}) \cdot g \cdot d_K}{\rho_{H_2\mathrm{O}} \cdot v_z^2} = \frac{4}{3} \frac{\mathrm{Eö}}{\mathrm{We}}, \tag{4}$$

where $v_z$ – average speed of a freely falling ball, Eö – Eötvös number, Eö $= \frac{(\rho_K - \rho_{\mathrm{H_2O}}) \cdot d_K^2}{\sigma}$, We – Weber number, We $= \frac{\rho_K \cdot d_K \cdot v_z^2}{\sigma}$, $\sigma$ – surface tension, $\rho_K$ – ball density.

## 3. Outline of the measuring set-up and research work

Research work was done using the set-up illustrated in Fig. 3, including a pneumatic system holding the balls and allowing the start of their free falling accurately in the centre of the tank, without using any additional forces.

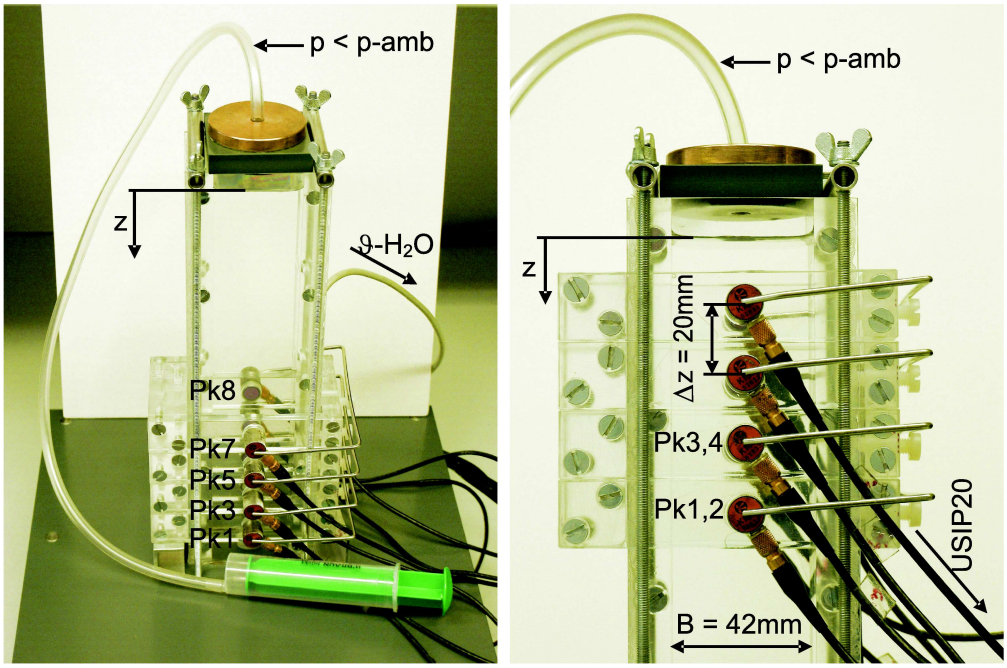


Fig. 3. Scheme of measuring set-up: p-amb – ambient pressure.

The 15 MHz ultrasonic sensors, Pk1–Pk8, are installed in four planes, at a distance $\Delta z = 20$ mm from each other on opposite sides of the measuring tank of square cross-section and width B $= 42$ mm. The tank was made of plexiglass to allow for direct falling paths of the balls. Using the characteristics shown in Fig. 4, the SH12 – level

was used as the measuring range of the ultrasonic flaw detector, hence the sensitivity coefficient was $K = 68$ µs/5 V. Such a value enabled us to determine the passage time for the second echo, $t_{2.\mathrm{RWE}}$, without any change in the measuring range.

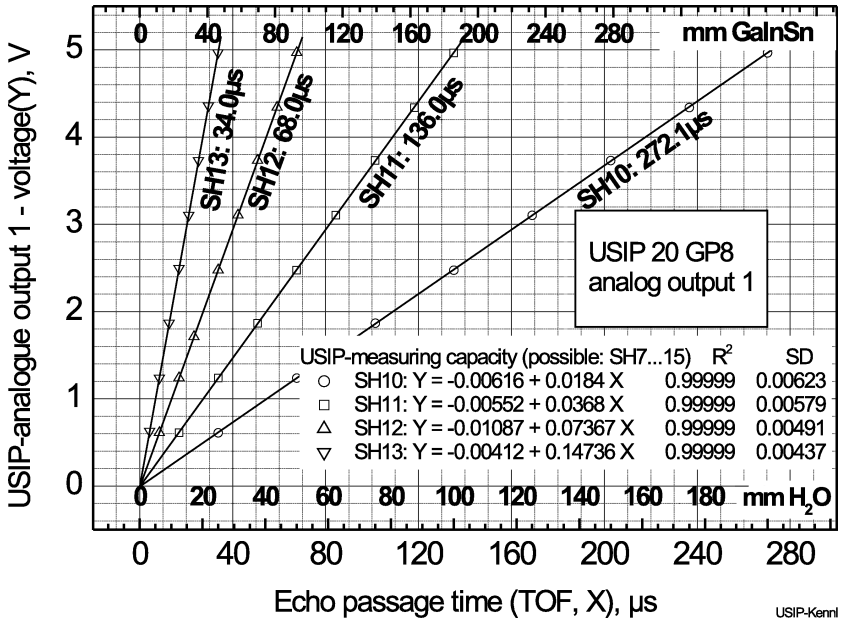


Fig. 4. Selected measuring ranges of ultrasonic flaw detector, type USIP 20 GP8: $R^2$ – correlation coefficient, SD – standard deviation.

Steel and glass balls with various diameters and densities, $\rho_K$, determined by multiple accurate measurements of their masses and by calculating their volumes, were selected for tests. Testing schedule was prepared so as to determine the values of the drag coefficients, $c_D$, of balls, both for the accelerated and uniform motion. For this reason, the measurements were taken at the top and at the bottom parts of the tank while reducing its filling with water to the level $z = 235$ mm. For this height, only the steel balls with diameters $d_K < 6.34$ mm have reached, at their final phase of travel, the stabilized velocity (calculated according to BRAUER [7] the path of acceleration for balls with diameter $d_K = 6.34$ mm, at the assumption that the start of uniform motion is determined by falling velocity equal to 95% of the final velocity, is $z_{\mathrm{soll}} = 195$ mm). The other falling balls were still performing accelerated motion. Several dozens of measurements were made for each freely falling ball, while the analysis was made for those balls only which fall along a straight line.

Only measuring time of flight of moving balls (L) and maximum available gain of signals were used in the research procedure.

For eight ultrasonic sensors used and at the pulse repetition frequency of 8,000 Hz (sampling frequency $\delta t = 1$ ms), the times of flight $(t_1, t_2) \ldots (t_7, t_8)$ in particular planes were not measured simultaneously but were shifted by 0.125 ms. For such a difference,

balls falling at velocity $v_z < 1$ m/s cover the distance $z < 0.12$ mm, and in the case of balls the diameter of which is larger than the width of ultrasonic field or balls being at its limit, there may occur some measurement errors. However, when the method will be used for liquid/gas two-phase flows, the expected velocity of moving-up bubbles is less than 0.3 m/s and the time shift of signals being received is of no practical effect for the method accuracy and it may be neglected. Limiting this problem to calculations of the ball diameter, the minimum value of time $t_1 + t_2$ in Eq. (1) is assumed.

One analogue output of the ultrasonic flaw detector, type USIP 20 GP8, was used to record the signals. Signals were sampled with the NI 6023E Card (200 kS/s, 12 bit) and with DASYLab software developed by DASYTEC Company. The ultrasonic field, generated in water by ultrasonic sensors, type K15K, used in testing, with the frequency $f = 15$ MHz and diameter $D = 5$ mm, featured the following specifications:

- near-field range $l_o = 63.1$ mm,
- beam divergence angle $\varphi \approx 1.4°$,
- ultrasonic wave length to sensor diameter ratio $\lambda/D = 0.0198$.

This ensured that, in practice, only the longitudinal wave was present over the entire width of the tank covered by the cylindrical ultrasonic field.

The speed of falling balls was calculated from the cross-correlation function of the signals – by determining the signal delay time $t_{KKF}$. For accurate calculations, the falling speed was assumed as the average of 4 correlation functions (e.g. Pk1–Pk3, Pk1–Pk4, Pk2–Pk4, Pk2–Pk3 as shown in Fig. 2).

In order to determine the ultrasonic wave velocity, water temperature was measured using a calibrated PT100 resistance thermometer with digital display.

## 4. Results of measurements

### *4.1. Diameter of freely falling balls*

Figure 5 illustrates the exemplary measurement signals together with the sum of times, $t_1+t_2$, and plots of signals in each measuring plane for falling glass ball 13.82 mm in diameter. The values of ball diameter are also calculated.

Summary results of the test carried out are shown in Fig. 6. It provides the following relationships:

- relative error of average ball diameters, together with type A standard uncertainty,
- type B standard uncertainty of ball diameters,

versus their real standard diameter $d_{\text{Soll}}$.

The measurement error was determined according to [8] as the percentage difference between the average values of ball diameters, obtained by measurements and their standard diameters. The reason for this was the assumption that the true value of ball diameters is equal to the standard value i.e., that ball diameters measurements made by means of caliper with a digital readout and resolution 0.01 mm were omitted (relative experimental standard deviation for a series of 20 measurements was $\sim$0% for steel balls, and less than 0.2% for glass balls).

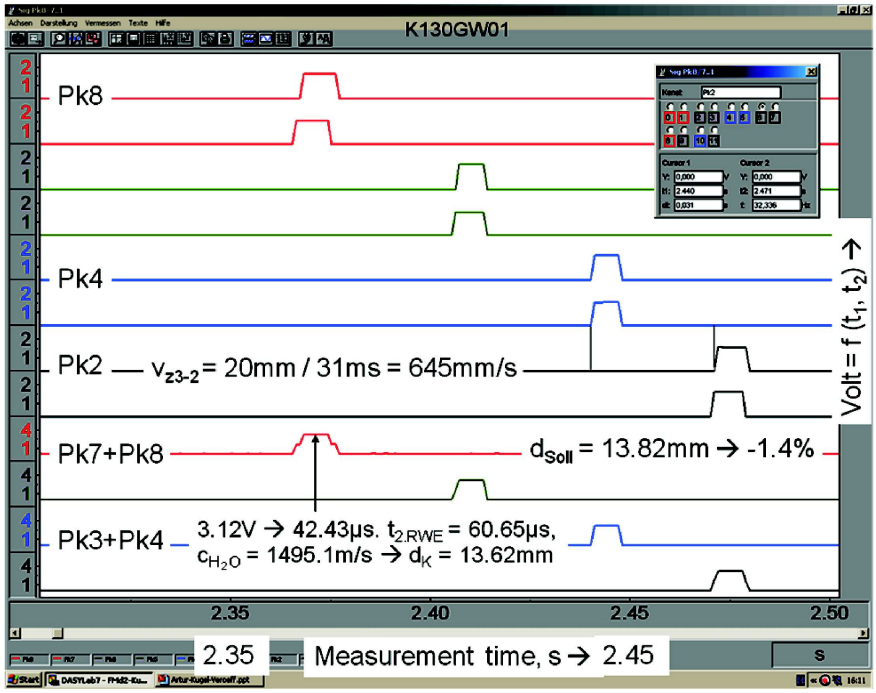


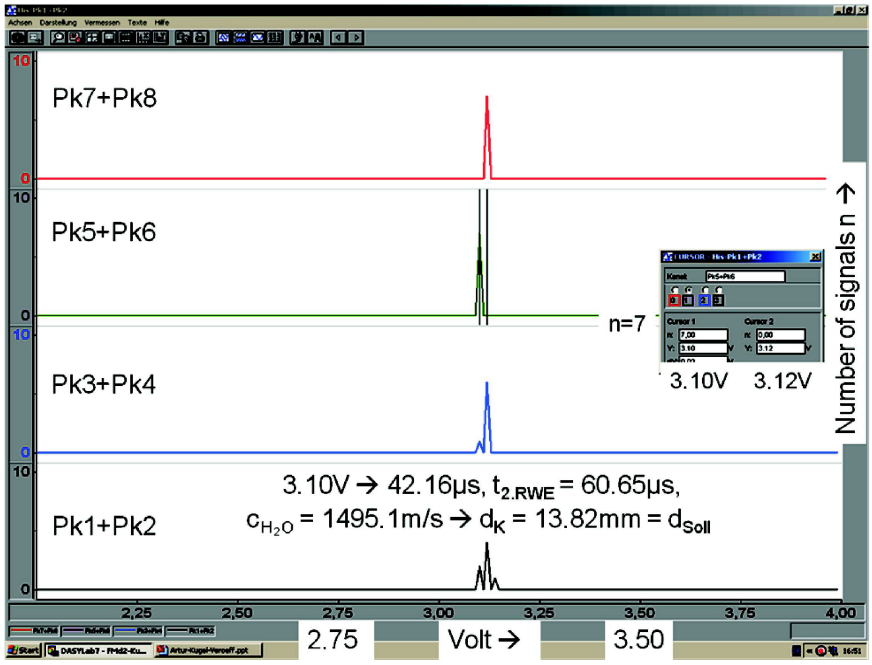


Fig. 5. Examples of recorded signals and plots for feely falling glass ball with diameter $d_{\mathrm{Soll}} = 13.82$ mm in various measuring planes.

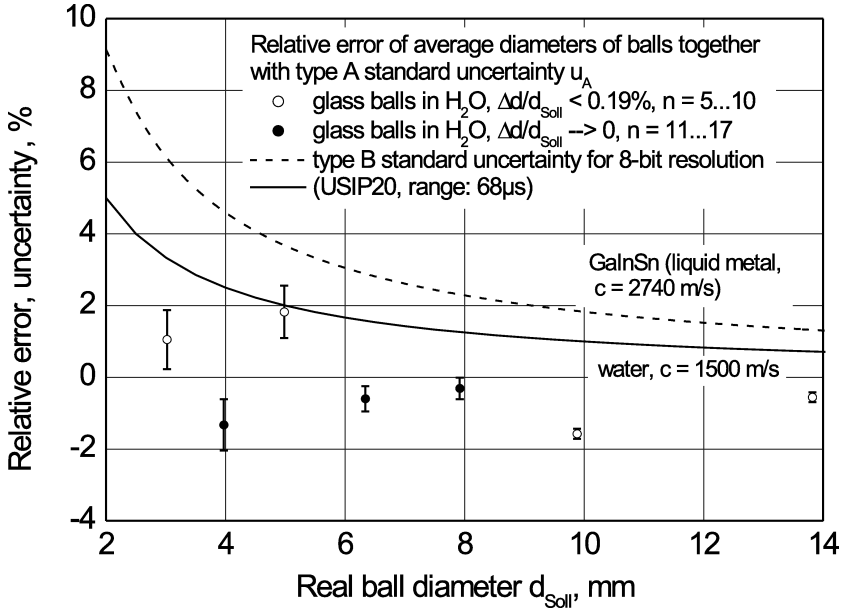


Fig. 6. Errors in determining diameters of the falling balls: $\Delta d = d_K - d_{\text{Soll}}$, $n$ – number of measurements.

Type B standard uncertainty for the falling ball diameter was determined by a direct method according to Eqs. (1) and (2), assuming that the second time of flight, $t_{2.\text{RWE}}$, is measured. For independence of all variables, it is given by Eq. (5):

$$\frac{u_{B_{d_K}}}{d_K} = \sqrt{\left(\frac{u_{B_{c_{\text{H}_2\text{0}}}}}{c_{\text{H}_2\text{0}}}\right)^2 + \left(\frac{u_{B_{t_{2.\text{RWE}}}}}{t_K}\right)^2 + \left(\frac{u_{B_{t_1}}}{t_K}\right)^2 + \left(\frac{u_{B_{t_2}}}{t_K}\right)^2}. \tag{5}$$

Because standard uncertainties of all passage times included in Eq. (3) are equal, it takes the following form:

$$\frac{u_{B_{d_K}}}{d_K} = \sqrt{\left(\frac{u_{B_{c_{\text{H}_2\text{0}}}}}{c_{\text{H}_2\text{0}}}\right)^2 + 3\left(\frac{u_{B_t}}{t_K}\right)^2}. \tag{6}$$

Component uncertainties of time, $t_K$, are related with a 8-bit D/A converter included in the USIP 20 GP defectoscope, and with later sampling the signals using 12-bit card, type NI 6023E (200 kS/s, 12 bit). Disregarding the quantization error of the NI 6023E Card and assuming only one component of uncertainty, the 8-bit converter, for the assumed coefficient of ultrasonic defectoscope sensibility $K = (68\ \mu\text{s/5 V})$, the resolution of the time of flight is $\delta t = 68\ \mu\text{s}/(2^8) \approx 266\ \mu\text{s}$, while the type B standard uncertainty according to GUM [8] is $u_{B_t} = \dfrac{\delta t}{\sqrt{12}} \approx 77$ ns.

In calculating the ultrasonic wave velocity in water, the equation given by WILSON [9] approximated by a fourth-order polynomial was assumed. In comparison with the most accurate Marczak equation [10] for the temperature range 10–40°C, the dif-

ferences in calculations of ultrasonic wave velocity are less than 0.037%, and when comparison is made with the recommended equation of Lubbers and Graaffs [10], they are within the interval $\langle -0.015\%,\ 0.010\% \rangle$. Thus, the main source of errors for determining the ultrasonic velocity in water is the temperature measurement using Pt100 resistance thermometer. Following calibration by means of a mercurial thermometer with 0.1 K readout resolution, the error not allowed for correction of PT100 resistance thermometer indications was 0.4°C.

Calculated from the equation of Lubbers and Graaffs of the form:

$$c_{\mathrm{H_2O}} = 1405.03 + 4.624 \cdot (\vartheta/^{\circ}\mathrm{C}) - 0.0383 \cdot (\vartheta/^{\circ}\mathrm{C})^2 \tag{7}$$

for water temperature during measurements $\upsilon = 25^{\circ}$C, the sensibility:

$$\frac{dc_{\mathrm{H_2O}}}{d\vartheta} = 4.624 - 0.0766 \cdot (\vartheta/^{\circ}\mathrm{C}) \tag{8}$$

is $\left(\dfrac{dc}{d\vartheta}\right)_{25^{\circ}\mathrm{C}} = 2.709$ m/s ·K. Thus, the correction of $0.4^{\circ}$C for temperature being measured causes additional error of ultrasonic wave velocity equal to 1.08 m/s which, when compared with the real value of 1496.69 m/s, may be neglected. Following transformations and disregarding the ultrasonic wave velocity uncertainty, the relative type-B standard uncertainty of the ball diameter under measurement is given by the equation:

$$\frac{u_{B_{d_K}}}{d_K} \cong \sqrt{3} \cdot \frac{u_{B_t}}{t_K} \cong \left(\frac{\sqrt{3}}{2}\right) \cdot \frac{c_{\mathrm{H_2O}} \cdot u_{B_t}}{d_K}. \tag{9}$$

Figure 6 illustrates also the relation of the type B relative standard uncertainty for the case when the tank is filled with liquid metal GaInSn. According to the relations given in diagram 6, it follows that when determining the dimensions of gas bubbles in motion, with diameter in the range of $\langle 4$ mm, 6 mm$\rangle$, for such a measuring system we should expect the uncertainty of co. 2.5% for bubbles moving upwards in water and about 4.4% for bubbles moving upwards in liquid metal GaInSn.

### *4.2. Frontal drag coefficient*

The values of frontal drag coefficient were determined from Eq. (4) assuming the ball velocity as an average obtained from correlation measurements at specific falling height. For a falling glass ball with diameter 13.82 mm, Fig. 7 shows exemplary cross-correlation functions for the measurement signals. It is also visible that for ultrasonic sensors installed in the upper part of the tank, the ball is still in the acceleration motion phase.

Figure 8 shows the relationship between the falling speed changes versus the distance covered, while Fig. 9 presents the overall measurement results. The values of drag coefficients for single spherical particles from Kaskas equation and for a circular disk [7] are shown in this figure as well.

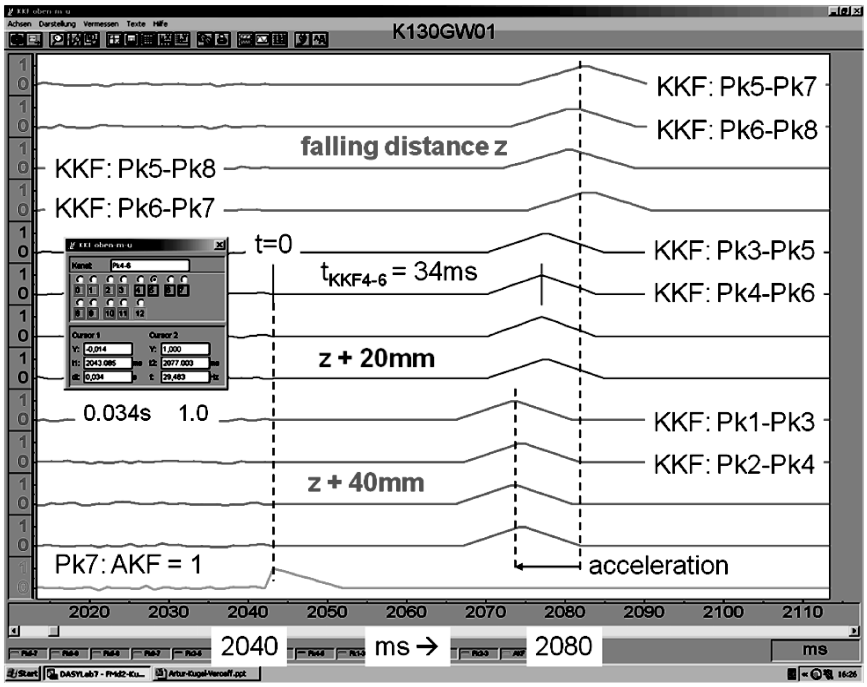


Fig. 7. Exemplary correlation functions for glass ball with diameter $d_{\mathrm{Soll}} = 13.82$ mm.

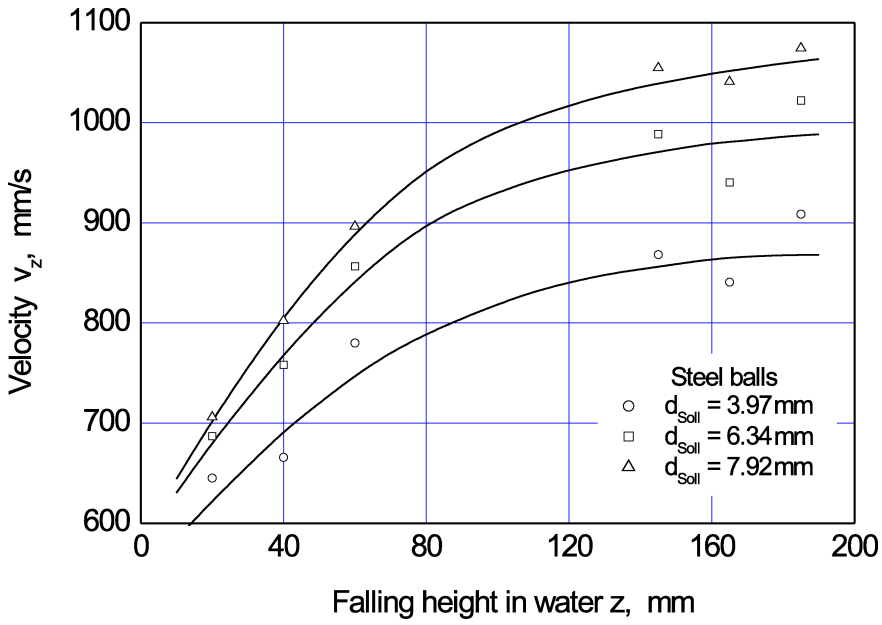


Fig. 8. Falling velocity variations versus distance covered by steel balls.

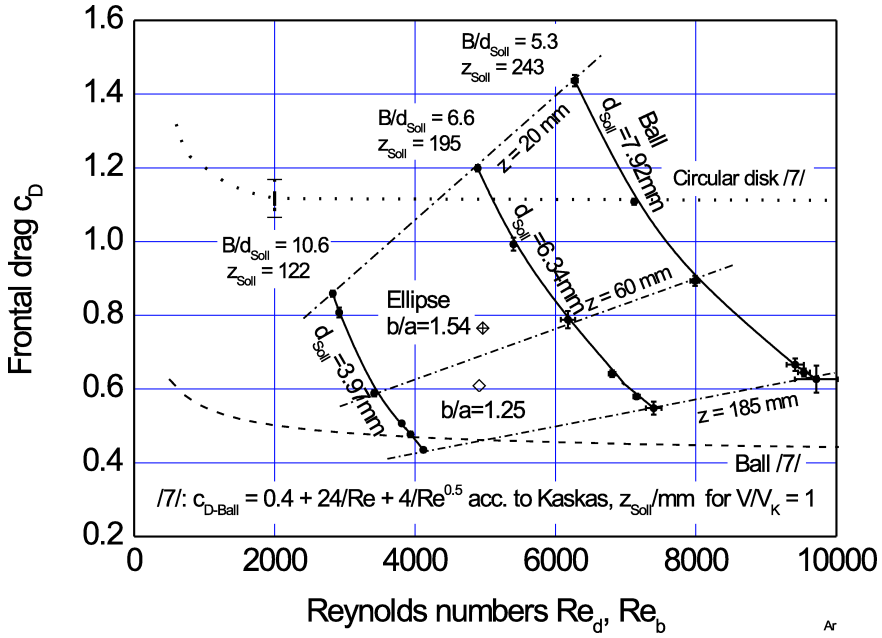


Fig. 9. Frontal drag of steel falling balls versus Reynolds number: $V$ – volume of liquid surrounding the ball and taking part in motion, $V_K$ – ball volume.

While the drag coefficient increases during the first stage of motion which is related to the zone of accelerated motion (lower falling velocity), only the steel ball with diameter $d_{\text{Soll}} = 3.97$ mm at measuring heights $z = 145/165/185$ mm reaches its fixed velocity and the values of drag coefficients are the same as those calculated from the Kaskas equation and are around 0.44. For the remaining balls, the differences between the two values are clearly distinguished. Higher values of frontal drag coefficients at bottom heights of falling are related to the influence of tank walls (for a ball with dimension $d_{\text{Soll}} = 6.34$ mm, the ratio $B/d_{\text{Soll}} = 6.6$, while for $d_{\text{Soll}} = 7.92$ mm this ratio is $B/d_{\text{Soll}} = 5.3$) and their accelerated motion being continued – this is clearly visible for the ball with diameter $d_{\text{Soll}} = 7.92$ mm (assuming, according to Brauer, the distance of acceleration is $z_{\text{Soll}} = 243$ mm), and the values of drag coefficient for this distance at the falling height $z = 185$ mm are around $c_D = 0.62$.

## 5. Conclusions

The ultrasonic/pulse echo method presented in the paper enables quite accurate determination of diameters for freely falling balls. Relative errors were not higher than 2%, while type B standard uncertainty related mainly with resolution of readouts for time of flight of balls with diameters above 4 mm tends to about 1%. Furthermore, determining the values of falling speed (e.g. with correlation functions), we may calculate the frontal drag coefficient. In case of steel balls with diameter $d_{\text{Soll}} = 3.97$ mm in

uniform motion, the calculated values of drag coefficient amounting to $c_D \approx 0.44$ were consistent with those obtained from the Kaskas theoretical equation. Hence, the method seems to be effectively used to determine the diameter and frontal drag coefficient of lifting gas bubbles, both in water and in liquid metals. Exemplary values of the drag coefficient were calculated for argon elliptic bubbles lifting in liquid metal GaInSn with and without the influence of longitudinal magnetic field.

## References

[1] ORZECHOWSKI Z., PRYWER J., ZARZYCKI R., *Fluid mechanics in environmental engineering* [in Polish]: *Mechanika płynów w inżynierii środowiska*, Wydawnictwa Naukowo-Techniczne, Warszawa 2001.

[2] KANTARCI N., BORAK F., ULGEN K.O., *Bubble column reactors*, Process Biochemistry, **40**, 2263–2283 (2005).

[3] KAISER E., *Elektromagnetischer Sensor zur Detektion der Flüssigkeits- und Gasbewegung bei aufsteigenden Basen in Flüssigmetall*, Technisches Messen, **71**, 349–357 (2004).

[4] KAISER E., *Wirbelstromsensoren als Blasendetektor in der Zweiphasenströmung Gas/Flüssigmetall*, Chemie-Ingenieur-Technik, **76**, 286–288 (2004).

[5] KAISER E., SOMMERLATT H.-D., ANDRUSZKIEWICZ A., *Ultrasonic method of measuring of a two-phase fluid-gas flow* [in Polish]: *Pomiary przepływu dwufazowego ciecz-gaz za pomocą metody ultradźwiękowej*, Metrologia w procesie poznania, Kongres Metrologii, Materiały kongresowe, pp. 283–286, Wrocław 6–9.09.2004.

[6] ANDRUSZKIEWICZ A., KAISER E., SOMMERLATT H.-D., *Adaptation of defectoscopic methods for identification of two-phase fluid-gas flows* [in Polish]: *Adaptacja metod defektoskopowych do identyfikacji przepływów dwufazowych ciecz-gaz*, Pomiary Automatyka Robotyka, **5**, 5–8 (2005).

[7] BRAUER H., *Grundlagen der Einphasen- und Mehrphasenströmungen*, Verlag Sauerländer, Aarau und Frankfurt am Main 1971.

[8] *Wyrażanie niepewności pomiaru. Przewodnik*, Główny Urząd Miar, 1999.

[9] WILSON W.D., *Equation for the Speed of Sound in Seawater*, J. Acoust. Soc. Am., **32**, 10, 1357 (1960).

[10] *Technical Guides- Speed of Sound In Pure Water,* National Physical Laboratory, Teddington, Middlesex, UK, TW11 0LW, 2000.